

Communication

# Multi-Wavelength Terahertz Parametric Generator Using a Seed Laser Based on Four-Wave Mixing

Sota Mine, Kodo Kawase and Kosuke Murate \*

Department of Electronics, Graduate School of Engineering, Nagoya University, Nagoya 464-8603, Japan; mine.sota@b.mbox.nagoya-u.ac.jp (S.M.); kawase@nuee.nagoya-u.ac.jp (K.K.)

\* Correspondence: murate@nuee.nagoya-u.ac.jp; Tel.: +81-52-789-3169

**Abstract:** In this study, we developed a multi-wavelength terahertz-wave parametric generator that operates with only one injection seeding laser. Tunable lasers used as an injection seeder must be single-frequency oscillators, and conventional multi-wavelength terahertz-wave parametric generator requires basically the same number of lasers as the number of wavelengths. In order to solve this problem, we developed a new external cavity semiconductor laser that incorporates a DMD in its wavelength-selective mechanism. In this process, stable multi-wavelength oscillation from a single laser was made possible by efficiently causing four-wave mixing. This seed laser can be applied to practical real-time terahertz spectroscopy by arbitrarily switching the desired wavelength to be generated and the interval between multiple wavelengths.

**Keywords:** terahertz; real-time identification; external cavity laser diode; four-wave mixing



**Citation:** Mine, S.; Kawase, K.; Murate, K. Multi-Wavelength Terahertz Parametric Generator Using a Seed Laser Based on Four-Wave Mixing. *Photonics* **2022**, *9*, 258. <https://doi.org/10.3390/photonics9040258>

Received: 24 March 2022

Accepted: 10 April 2022

Published: 12 April 2022

**Publisher's Note:** MDPI stays neutral with regard to jurisdictional claims in published maps and institutional affiliations.



**Copyright:** © 2022 by the authors. Licensee MDPI, Basel, Switzerland. This article is an open access article distributed under the terms and conditions of the Creative Commons Attribution (CC BY) license (<https://creativecommons.org/licenses/by/4.0/>).

## 1. Introduction

Real-time measurement/spectroscopy is expected to be realized for terahertz-wave applications. In the sub-THz region, real-time measurement products such as scanners and cameras using a fixed frequency have been commercialized [1–4], but there are still few practical systems in the 1~3 THz region. For this reason, methods using an injection seeded terahertz parametric generator (is-TPG), which excels at measurements through shielding, have been studied [5]. Recently, we investigated real-time spectroscopy using simultaneous multi-wavelength generation from is-TPGs [6] and fast wavelength sweep [7]. Is-TPG is a device that generates terahertz waves corresponding to the difference frequency of two laser beams injected into a MgO:LiNbO<sub>3</sub> crystal: an intense pulse of pump beam and a continuous wave (CW) injection seeding beam. Not only can it generate high-intensity, widely tunable terahertz-waves, but it also achieves a wide dynamic range of 125 dB in combination with parametric detection of the inverse process [8]. Furthermore, we are exploring various applications of machine learning in terahertz spectroscopy, such as the detection of illicit drugs in envelopes [9] and terahertz tag measurements [10].

## 2. Experimental Method

### 2.1. Multiwavelength Generation from is-TPG

Excitation of MgO:LiNbO<sub>3</sub> (hereafter, called as LiNbO<sub>3</sub>) with a high intensity laser causes parametric down conversion (parametric fluorescence) due to spontaneous Raman scattering via polariton, which is coupling between phonons and terahertz waves (photons). This generates a terahertz wave and near infrared light (Stokes beam) with a wavelength slightly different from the pump beam [11]. As these lights propagate through the crystal, they are amplified by parametric interactions and broadband terahertz wave output is obtained. This terahertz generation scheme is called terahertz-wave parametric generation (TPG). On the other hand, TPG with injection seeding is called is-TPG [5]. In is-TPG, wide tunability of the generated terahertz wave is obtained by varying the wavelength and

incident angle of the seed beam to satisfy the non-collinear phase matching condition. This means that the wavelength to be amplified from the broadband light generated by the parametric fluorescence is selected by injection seeding. Hence, if multiple seed beams are injected, the wavelength at which the gain is concentrated can be divided into multiple wavelengths. This enables multi-wavelength terahertz wave generation from is-TPG [6]. However, it is generally difficult to stably oscillate a multi-wavelength CW beam from a laser, and the multi-wavelength seed source near 1070 nm that we seek is not commercially available and is difficult to develop. Conventionally, multiple ECLDs (external cavity laser diodes) have been combined as a multi-wavelength seed source [6], but it has been difficult to further increase the number of wavelengths because the same number of lasers are required. In this study, however, an ECLD using a digital micromirror device (DMD) as a wavelength-selective mechanism stably generates multiple wavelengths by utilizing the four-wave mixing that occurs inside the ECLD. We introduced it as a seed source of is-TPG, and developed a wavelength-switchable multi-wavelength terahertz-wave parametric generator.

### *2.2. Multi Wavelength Seed Laser Based on Four-Wave Mixing*

An ECLD is a longitudinal mode-controlled semiconductor laser, also called an ECDL (referred to as an ECLD in this paper). Wavelength tunability is achieved by setting up an external cavity outside the semiconductor laser (LD) and selecting the wavelength to be fed back by a diffraction grating and mirror. Compared to DFB lasers [12] and surface emitting semiconductor lasers (VCSELs) [13], which control longitudinal modes with the LD itself, wideband wavelength tunability, narrow linewidths below MHz, and mode hop-free operation can be realized. However, general ECLDs are single-wavelength oscillators because the light dispersed by the diffraction grating is selected by the angle of the mirror, making simultaneous multi-wavelength oscillation difficult.

In this study, we use a DMD as a wavelength selection mechanism, which is a device consisting of an array of microscopic mirrors. The DMD chip used in this study is a Texas Instruments dlp4500NIR, which consists of  $1140 \times 912$  micro mirrors of  $7.6 \mu\text{m}$  square, each of which has a binary angle of  $\pm 12^\circ$  due to electrostatic forces. An AJD-4500 from Ajile was used to control the DMD chip. The ECLD is shown on the left side of Figure 1, where the amplified spontaneous emission (ASE) output from the LD is wavelength resolved by a grating and is focused onto the DMD by a lens [14–19]. At this time, by placing the grating and DMD at both focal points of the lens, each wavelength is focused onto the DMD surface in a spatially separated state. Therefore, by controlling the mirror at the location corresponding to the wavelength to be output among the micro mirrors on the DMD, the system operates as an ECLD. In order to suppress spatial hole-burning [20], which leads to instability in power and oscillation wavelength, a ring cavity instead of a Fabry–Perot type is used for the external resonator. By using oscillation with a unidirectional traveling wave, standing waves are not generated and longitudinal mode fluctuations due to spatial hole-burning are suppressed. In a Fabry–Perot type resonator, not only the wavelength-selected light but also the ASE returns to the LD, so the two light sources compete for gain and efficiency drops. On the other hand, in a ring cavity, only wavelength-selected light returns to the LD, resulting in efficient oscillation. For the same reason, as the ASE does not lead to laser output, an ASE-free high S/N is realized.

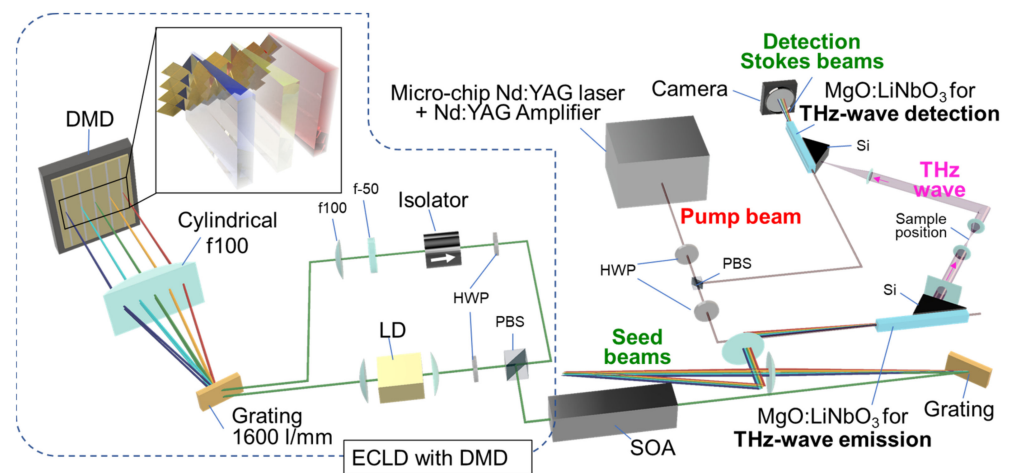


**Figure 1.** Multi-wavelength terahertz-wave parametric generator using multi-wavelength ECLD as an injection seeding source.

We have reported on the fast wavelength tunability [21] and terahertz wave generation [7] using this laser, which shows excellent characteristics as an injection source of is-TPG due to its fast speed of more than 6 kHz and high S/N, and also shows an excellent performance for wavelength tunability. The new system enables a significant increase in speed. In this study, we will apply this laser’s ability to select arbitrary wavelengths to achieve simultaneous multi-wavelength oscillation. Simply put, simultaneous multi-wavelength oscillation can be achieved by reflecting multiple wavelengths simultaneously by a DMD [16]. However, the problem with simultaneous multi-wavelength oscillation from a single gain chip is mode competition (gain competition), which occurs when multiple wavelengths compete for gain. Mode competition also occurs in simultaneous multi-wavelength oscillation using this ECLD, resulting in problems such as reduced stability, increased line width, and no single-mode oscillation.

A method to suppress this mode competition and achieve simultaneous multi-wavelength oscillation is to use four-wave mixing [22]. When a signal beam and a pump beam are injected into a nonlinear optical crystal, an idler beam is generated, as shown in this equation,

$$f_{idler} = f_{pump_1} + f_{pump_2} - f_{signal}$$

and the generation efficiency is higher when the frequency difference between the input beams is small and the light intensity oscillations due to interference are small, because four-wave mixing in semiconductor lasers originates from time fluctuations in the carrier density. When the pump beam has one wavelength, it is called degenerate four-wave mixing, and when it has two wavelengths, it is called nondegenerate four-wave mixing.

In conventional multi-wavelength lasers using four-wave mixing, the generated idler beam behaves as a pump beam to generate a new idler beam so as to generate light with evenly spaced wavelengths over a wide bandwidth. On the other hand, in the multi-wavelength laser we developed, we focused on the interaction of the pump beam and idler beam, and used four-wave mixing as a measure to suppress mode competition between wavelengths selected by the DMD. When four-wave mixing occurs and a light beam already exists at the wavelength where the idler beam was generated, the existing light is optically parametrically amplified. When four or more wavelengths of beam are input and four-wave mixing occurs, all wavelengths become idler beam from the perspective of one of the wavelength component pairs, so they are mutually amplified and mode competition can be suppressed. Furthermore, four-wave mixing generates an idler beam component that is not part of the incident wavelength component, but as shown in Figure 2, the unwanted beam can be spatially blocked by the DMD. In addition, as the center wavelength at which

four-wave mixing occurs is variable by using DMD, not only the number of wavelengths generated but also the wavelengths can be arbitrarily controlled.

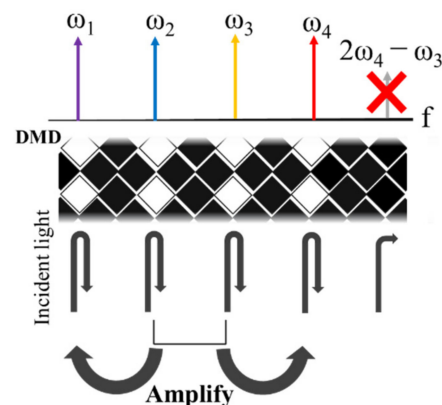


**Figure 2.** Four-wave mixing is generated by reflecting equally spaced wavelengths. Unwanted wavelength components can be blocked by the DMD.

In order to efficiently generate four-wave mixing, we made the following modifications to the gain medium, power density, and longitudinal mode fluctuations in this laser. The semiconductor laser (OE-1040TA; Spectra Quest Lab, Inc., Chiba, Japan) made of InGaAs and AlGaAs used in this study had a few-micron-size aperture and total length of 4 mm, which allowed for a high efficiency and longer nonlinear interaction length, thus facilitating nonlinear optical effects. Next, although four-wave mixing is more likely to occur at higher power densities, the damage threshold of the DMD is low and the power density in the resonator is limited, so a cylindrical lens was used to inject the DMD. Finally, regarding longitudinal mode fluctuations, when a Fabry–Perot type resonator is introduced into an external resonator, standing waves are generated in the resonator, causing spatial hole-burning that results in fluctuations in the longitudinal mode. When the wavelength component becomes unstable, the phase matching condition for four-wave mixing is not satisfied, and the generation is inhibited. Therefore, as mentioned above, a ring cavity was introduced in the external resonator. In using four-wave mixing, in which the interaction between wavelengths is important, we considered it desirable to orient the DMD so that the distance between the micro-mirror and the focusing lens was uniform for all wavelength components. Therefore, we conducted experiments in a vertical configuration in which the rotation axis of the micro-mirror was in the wavelength-resolved direction, which was 90 degrees different from the orientation selected for single-mode oscillation [21].

### 3. Results

#### 3.1. Multi Wavelength Output from ECLD

Figure 3 shows the spectrum of simultaneous multi-wavelength generation without four-wave mixing (measured with Advantest, Q8384). Three wavelength components that were not equally spaced were selected by the DMD and fed back into the resonator. When only one wavelength component was magnified and observed, it was confirmed that the line width was wide and no single-mode oscillation was observed. As mode competition among the three wavelengths was considered to be the cause, the correlation between the outputs of each wavelength was obtained. However, as all wavelengths were output coaxially, the output was injected into a diffraction grating to spatially separate each wavelength. Those lights were detected simultaneously using a camera to obtain the temporal variation of each wavelength intensity. As a result, the stability of each wavelength was 3.15%, 3.36%, and 3.61%, as shown in Figure 4. As there was some negative correlation coefficient of  $-0.4$  between the 1071.84 nm component, which had the highest output, and the other two wavelengths, mode competition is considered to be the cause of the stability deterioration. In addition, oscillation at four or more wavelengths was difficult because the gain was concentrated at one wavelength.

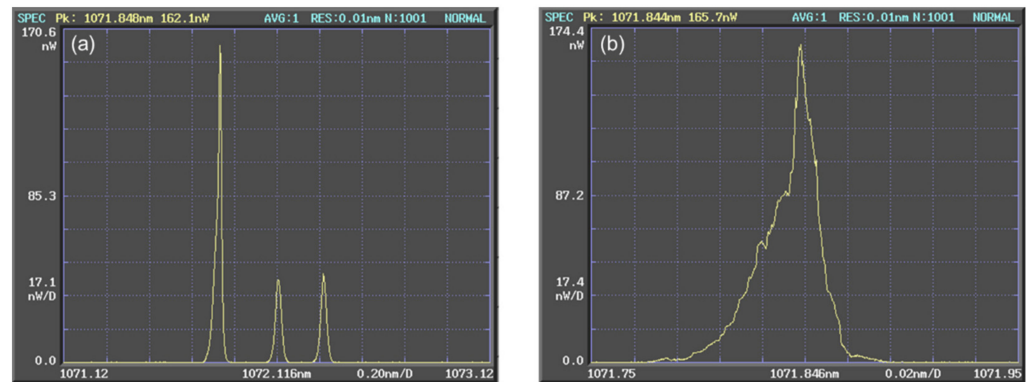


**Figure 3.** (a) Simultaneous generation of three wavelengths without four-wave mixing (0.20 nm/div). (b) Magnified view of only one wavelength (0.02 nm/div). The line width is thick and no single-mode oscillation is observed.

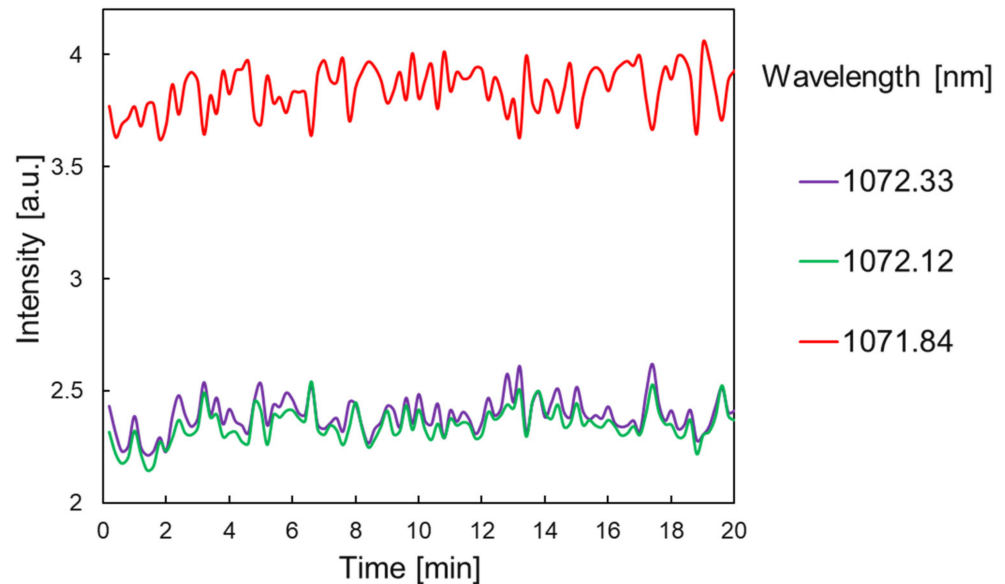


**Figure 4.** Stability graph of three-wavelength generation without four-wave mixing. The red line with the strongest intensity (1071.84 nm) and the intensities of the other two wavelengths are inversely proportional.

Next, Figure 5 shows the results of multi-wavelength oscillation using four-wave mixing, in which equally spaced light at five wavelengths was reflected by the DMD, causing four-wave mixing inside the semiconductor laser. When only one wavelength component was magnified and observed, the longitudinal mode oscillated in a single mode, as in the case of single-wavelength oscillation. In addition, as shown in Figure 6, the stability improved to 0.65%, 1.03%, 1.24%, 0.48%, and 1.23% in order from the shortest to longest wavelength. No negative correlation was observed for all of the wavelength pairs, suggesting that mode competition was suppressed. In addition, simultaneous oscillation was observed at up to 11 wavelengths, as shown in Figure 7. The distance between wavelengths could also be set arbitrarily by using DMD, and was tunable from 0.1 to 0.36 nm. The intensity difference of each wavelength component was varied by changing the wavelength, which is considered to be dependent on the gain of the semiconductor laser. In order to cause four-wave mixing in this laser, the power density inside the LD must be sufficiently high, and the excitation current of the LD was set to about 2000 mA. If a normal plano-convex lens is used to focus the light onto the DMD, 2000 mA excitation is not possible due to damage to the DMD, but we solved this problem by introducing a cylindrical lens as described above.

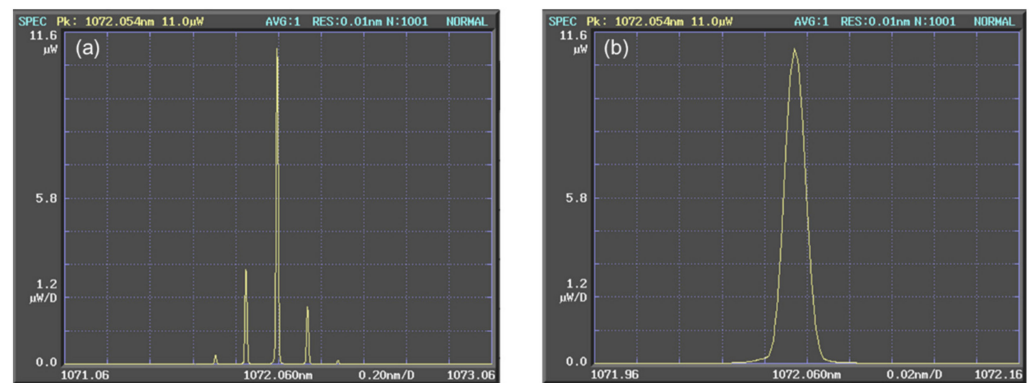


**Figure 5.** (a) Five-wavelength generation based on four-wave mixing (0.20 nm/div). (b) Enlarged view of only one wavelength, showing longitudinal single-mode oscillation. The vertical axes in (a,b) are a linear scale.

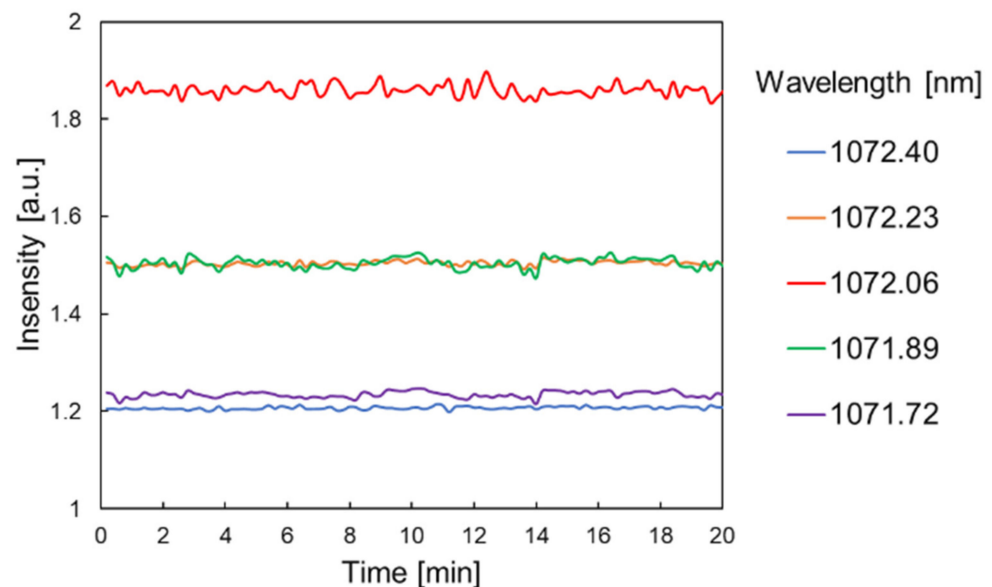


**Figure 6.** Stability of five-wavelength generation based on four-wave mixing.

### 3.2. Multi Wavelength THz Wave Generation from *is*-TPG

In fact, as shown in Figure 1, this laser was used as an injection source of *is*-TPG and simultaneous generation of multi-wavelength terahertz waves was attempted. Terahertz-wave parametric detection [8] was used for the detection. Terahertz waves were injected into the LiNbO<sub>3</sub> crystal for detection, together with the pump beam to upconvert the terahertz waves to near-infrared beam, which was then detected by a camera. The angle of emission differed for each wavelength according to the non-collinear phase matching condition, so that each wavelength could be captured by the camera separately. As shown in Figure 8, when five wavelengths were injected using four-wave mixing, it was confirmed that simultaneous generation of four wavelengths of terahertz waves was possible. Note that 1.35 THz, which corresponds to the fifth wavelength, was not observed here because its intensity was weak and was buried by the broadband noise. When the pump beam becomes stronger, parametric fluorescence also generates a non-injected broadband light from the LiNbO<sub>3</sub> crystal, which is called terahertz parametric generation (TPG) noise [23].

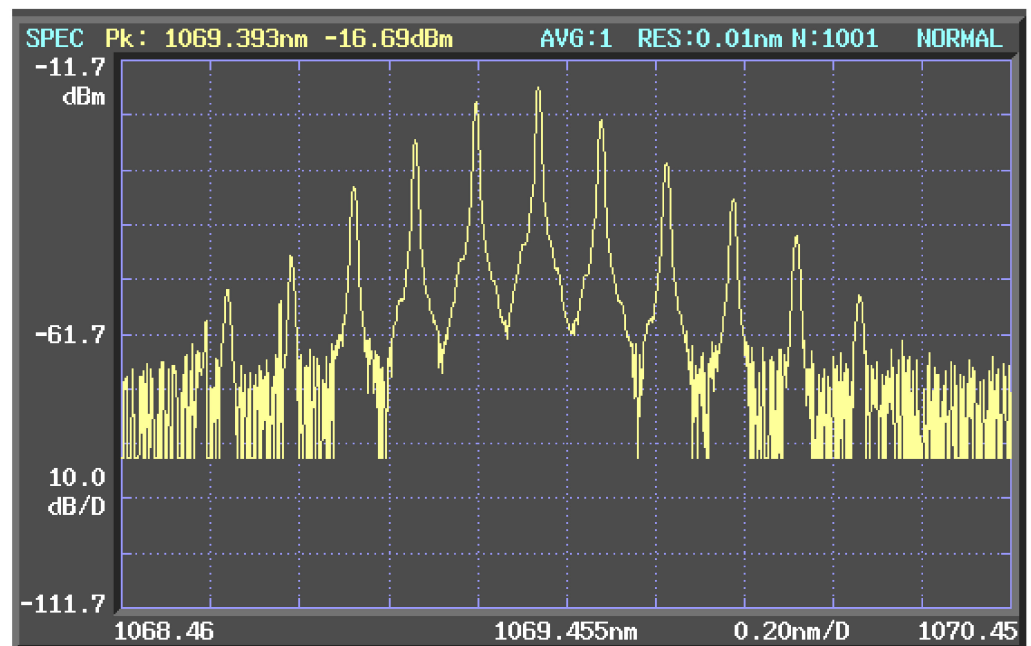


**Figure 7.** Simultaneous oscillation of 11 wavelengths.

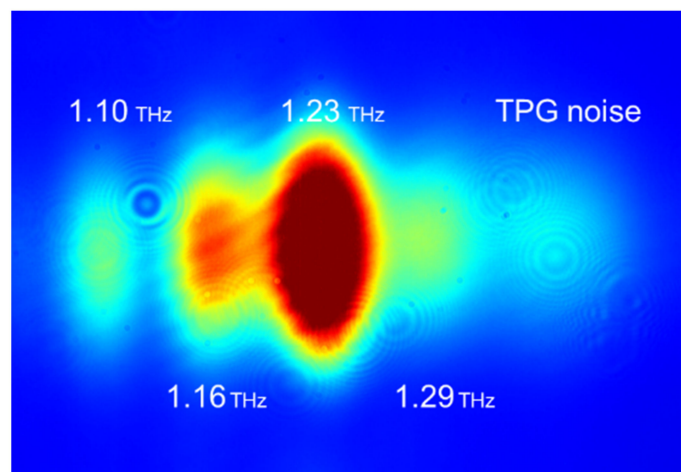


**Figure 8.** Simultaneous generation of four wavelengths from is-TPG using a multi-wavelength ECLD as an injection seeding source. Terahertz-wave parametric detection was used to upconvert the THz-waves to near-infrared beams.

Next, real-time spectroscopy was performed using multi-wavelength terahertz wave generation. In this case, there was a concern that the intensity difference of the injection seeding source would be reflected in the intensity difference of the terahertz wave, which would adversely affect the spectroscopic results. Therefore, an  $\text{Al}(\text{OH})_3$  pellet with a strong absorption peak at 1.23 THz was placed in the terahertz wave optical path and was used as a filter to flatten the intensity, so that the intensities were roughly aligned, as shown in Figure 9a. The reagents used for spectroscopy were maltose and  $\text{Al}(\text{OH})_3$ , which have absorption peaks at 1.13 THz and 1.23 THz, respectively. Spectroscopic measurements were performed over two sheets of cardboard and, as shown in Figure 9b,c, the intensity decay was found to be consistent with the absorption peaks of the substances.

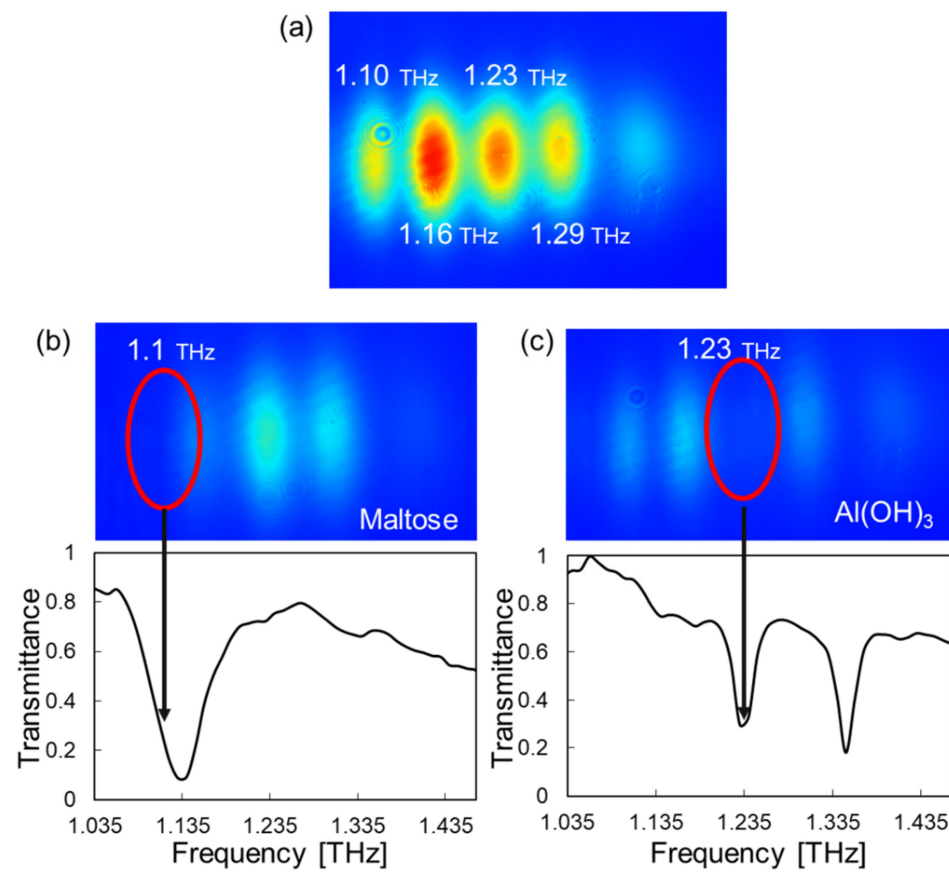


**Figure 9.** Reagent spectral results. (a) Reference with no sample inserted (output flattened by filter) (b) One-shot spectra of maltose and (c) Al(OH)<sub>3</sub> and their reference spectra.

#### 4. Discussion

In this study, the intensity differences between the generated terahertz wavelengths were aligned by inserting filters. However, this method cannot be used when the wavelength changes. Therefore, we plan to introduce two different methods. The first method is to control the number of mirrors on DMD to be reflected when we select the wavelength. In this study, the same number of mirrors were used for all wavelengths because stabilization and single-mode oscillation are essential. However, in the future, we would like to control the number of pixels in the horizontal and vertical directions of the DMD according to the difference in oscillation intensity of each wavelength. The second method is filtering by DMD externally rather than inside the ECLD. When the laser from ECLD is used as a seed source in is-TPG, an achromatic optical setup using a grating and lens pair is used to automatically control the angle of incidence for each wavelength, as shown in Figure 1. As each wavelength is spatially separated in this optical path, a DMD is inserted here to control the intensity of each wavelength in the same way as the method inside the ECLD. Through these improvements, we hope to make the system more practical.

#### 5. Conclusions

By modifying the resonator configuration of the ECLD used as a multi-wavelength injection seeding source for is-TPG, stable multi-wavelength oscillation has been achieved by efficiently generating four-wave mixing and suppressing gain competition even at multiple wavelengths. ECLD has been confirmed to oscillate up to 11 wavelengths, and the center wavelength and wavelength spacing can be arbitrarily controlled by the DMD. When used as an injection seeding source for is-TPG, simultaneous generation of four wavelengths was observed, indicating the possibility of a one-shot spectroscopy system with arbitrary switching of oscillation wavelengths and wavelength spacing. There has

been no report of multi-wavelength terahertz-wave generation using a single injection seeding source, and we expect that this system will contribute to making the system more compact, simpler, and less expensive.

**Author Contributions:** Conceptualization, K.M.; methodology, S.M. and K.M.; software, S.M.; formal analysis, S.M.; data curation, S.M. and K.M.; writing—original draft preparation, S.M. and K.M.; writing—review and editing, K.K. and K.M.; visualization, S.M. and K.M.; supervision, K.M.; project administration, K.M.; funding acquisition, K.K. and K.M. All authors have read and agreed to the published version of the manuscript.

**Funding:** This work was partially supported by the Japan Society for the Promotion of Science KAKENHI, grant numbers 18H03887 and 19H02627; Foundation of Public Interest of Tatematsu; and The Naito Science and Engineering Foundation.

**Institutional Review Board Statement:** Not applicable.

**Informed Consent Statement:** Not applicable.

**Data Availability Statement:** The data presented in this study are available on request from the corresponding author.

**Acknowledgments:** The authors appreciate the fruitful discussions with K. Muro and D. Fukuoka of Spectra Quest Lab, Inc. (<https://spectraquestlab.com/index.html>, accessed on 5 April 2022).

**Conflicts of Interest:** The authors declare no conflict of interest.

## References

1. Harris, Z.B.; Khani, M.E.; Arbab, M.H. Terahertz Portable Handheld Spectral Reflection (PHASR) Scanner. *IEEE Access* **2020**, *8*, 228024–228031. [[CrossRef](#)]
2. Suzuki, D.; Oda, S.; Kawano, Y. A Flexible and Wearable Terahertz Scanner. *Nat. Photonics* **2016**, *10*, 809–813. [[CrossRef](#)]
3. Zdanevičius, J.; Bauer, M.; Boppel, S.; Palenskis, V.; Lisauskas, A.; Krozer, V.; Roskos, H.G. Camera for High-Speed THz Imaging. *J. Infrared Millim. Terahertz Waves* **2015**, *36*, 986–997. [[CrossRef](#)]
4. Trichopoulos, G.C.; Mosbacher, H.L.; Burdette, D.; Sertel, K. A Broadband Focal Plane Array Camera for Real-Time THz Imaging Applications. *IEEE Trans. Antennas Propag.* **2013**, *61*, 1733–1740. [[CrossRef](#)]
5. Murate, K.; Kawase, K. Perspective: Terahertz Wave Parametric Generator and Its Applications. *J. Appl. Phys.* **2018**, *124*, 160901. [[CrossRef](#)]
6. Murate, K.; Hayashi, S.; Kawase, K. Multiwavelength Terahertz-Wave Parametric Generator for One-Pulse Spectroscopy. *Appl. Phys. Express* **2017**, *10*, 032401. [[CrossRef](#)]
7. Mine, S.; Kawase, K.; Murate, K. Real-Time Wide Dynamic Range Spectrometer Using a Rapidly Wavelength-Switchable Terahertz Parametric Source. *Opt. Lett.* **2021**, *46*, 2618–2621. [[CrossRef](#)]
8. Sakai, H.; Kawase, K.; Murate, K. Highly Sensitive Multi-Stage Terahertz Parametric Detector. *Opt. Lett.* **2020**, *45*, 3905–3908. [[CrossRef](#)]
9. Murate, K.; Kanai, H.; Kawase, K. Application of Machine Learning to Terahertz Spectroscopic Imaging of Reagents Hidden by Thick Shielding Materials. *IEEE Trans. Terahertz Sci. Technol.* **2021**, *11*, 620–625. [[CrossRef](#)]
10. Mitsuhashi, R.; Murate, K.; Niijima, S.; Horiuchi, T.; Kawase, K. Terahertz Tag Identifiable through Shielding Materials Using Machine Learning. *Opt. Express* **2020**, *28*, 3517–3527. [[CrossRef](#)]
11. Henry, C.H.; Garrett, C.G.B. Theory of Parametric Gain near a Lattice Resonance. *Phys. Rev.* **1968**, *171*, 1058–1064. [[CrossRef](#)]
12. Ghafouri-Shiraz, H.; Chu, C.Y.J. Distributed Feedback Lasers: An Overview. *Fiber Integr. Opt.* **1991**, *10*, 23–47. [[CrossRef](#)]
13. Michalzik, R. VCSELs: A Research Review. In *VCSELs*; Springer: Berlin/Heidelberg, Germany, 2013; pp. 3–18.
14. Riza, N.; Mughal, M.J. Broadband Optical Equalizer Using Fault Tolerant Digital Micromirrors. *Opt. Express* **2003**, *11*, 1559. [[CrossRef](#)] [[PubMed](#)]
15. Riza, N.A.; Ghauri, F.N. Hybrid Analog-Digital MEMS Fiber-Optic Variable Attenuator. *IEEE Photonics Technol. Lett.* **2005**, *17*, 124–126. [[CrossRef](#)]
16. Duncan, W.M.; Bartlett, T.; Lee, B.; Powell, D.; Rancuret, P.; Sawyers, B. Dynamic Optical Filtering in DWDM Systems Using the DMD. *Solid-State Electron.* **2002**, *46*, 1583–1585. [[CrossRef](#)]
17. Breede, M.; Kasseck, C.; Brenner, C.; Gerhardt, N.C.; Hofmann, M.; Hofling, R. Micromirror Device Controlled Tunable Diode Laser Diode Laser. *Electron. Lett.* **2007**, *43*, 456–457. [[CrossRef](#)]
18. Ai, Q.; Chen, X.; Tian, M.; Yan, B.; Zhang, Y.; Song, F.; Chen, G.; Sang, X.; Wang, Y.; Xiao, F. Demonstration of Multi-Wavelength Tunable Fiber Lasers Based on a Digital Micromirror Device Processor. *Appl. Opt.* **2015**, *54*, 603–607. [[CrossRef](#)]
19. Shin, W.; Lee, Y.L.; Yu, B.-A.; Noh, Y.-C.; Ahn, T.-J. Wavelength-Tunable Thulium-Doped Single Mode Fiber Laser Based on the Digitally Programmable Micro-Mirror Array. *Opt. Fiber Technol.* **2013**, *19*, 304–308. [[CrossRef](#)]

20. Pérez-Serrano, A.; Javaloyes, J.; Balle, S. Longitudinal Mode Multistability in Ring and Fabry-Pérot Lasers: The Effect of Spatial Hole Burning. *Opt. Express* **2011**, *19*, 3284–3289. [[CrossRef](#)]
21. Mine, S.; Kawase, K.; Murate, K. High-Power ASE-Free Fast Wavelength-Switchable External Cavity Diode Laser. *Appl. Opt.* **2021**, *60*, 1953–1957. [[CrossRef](#)]
22. Han, Y.-G.; Lee, S.B. Room-Temperature Tunable Multiwavelength Erbium-Doped Fiber Laser Based on Degenerate Four-Wave Mixing Effect in Dispersion-Shifted Fiber. In Proceedings of the Optical Fiber Communication Conference and Exposition and The National Fiber Optic Engineers Conference (2006), Anaheim, CA, USA, 5–10 March 2006; Paper OWI38. Optica Publishing Group: Anaheim, CA, USA, 2006.
23. Mine, S.; Kawase, K.; Murate, K. Noise-free terahertz-wave parametric generator. *Opt. Lett.* **2022**, *47*, 1113–1116. [[CrossRef](#)] [[PubMed](#)]